NASA
TM
82598
c.1

DOE/NASA/12726-7
NASA TM-82598

(NASA-TM-82598) PUMPING POWER CONSIDERATIONS IN THE DESIGNS OF NASA-REDOX FLOW CELLS Final Report (NASA) 12 p
HC A02/MF A01 CSCL 10C N81-26519
Unclas
G3/44 26981

Pumping Power Considerations in the Designs of NASA-Redox Flow Cells

LOAN COPY: RETURN TO
AFWL TECHNICAL LIBRARY
KIRTLAND AFB, N.M. 87117

Mark A. Hoberecht
National Aeronautics and Space Administration
Lewis Research Center

June 1981

Prepared for
U.S. DEPARTMENT OF ENERGY
Conservation and Renewable Energy
Division of Energy Storage Systems

TECH LIBRARY KAFB, NM

0150567

NOTICE

This report was prepared to document work sponsored by the United States Government. Neither the United States nor its agent, the United States Department of Energy, nor any Federal employees, nor any of their contractors, subcontractors or their employees, makes any warranty, express or implied, or assumes any legal liability or responsibility for the accuracy, completeness, or usefulness of any information, apparatus, product or process disclosed, or represents that its use would not infringe privately owned rights.

DOE/NASA/12726-7
NASA TM-82598

Pumping Power Considerations in the Designs of NASA-Redox Flow Cells

Mark A. Hoberecht
National Aeronautics and Space Administration
Lewis Research Center
Cleveland, Ohio 44135

June 1981

Work performed for
U.S. DEPARTMENT OF ENERGY
Conservation and Renewable Energy
Division of Energy Storage Systems
Washington, D.C. 20585
Under Interagency Agreement DE-AI04-80AL12726

SUMMARY

The NASA-Redox Energy Storage system uses two fully soluble redox couples as anode and cathode fluids. Both fluids are pumped through a redox cell, or stack of cells, where the electrochemical reactions take place at porous carbon felt electrodes. Pressure-drop losses are therefore associated with this system due to the continuous flow of reactant solutions. The exact pressure drop within a redox flow cell is directly dependent on the flow rate as well as the various cell dimensions.

Pumping power requirements for a specific set of cell operating conditions can be found for various cell geometries once the flow rate and pressure drop have been determined. Since these pumping power requirements contribute to the overall system parasitic energy losses which must be minimized, the choice of cell geometry becomes critical. Pressure-drop data for six different cell geometries of various flow port, manifold, and cavity dimensions are presented and discussed.

INTRODUCTION

One of the features of the NASA-Redox Energy Storage System is the requirement for continuous flow of the reactant solutions. Acidic iron chloride and chromium chloride are the reactant species that are circulated between two individual storage tanks and the power conversion section of the system, the redox stack (ref. 1). This stack can consist of any number and size of operational cells, depending on system voltage and current requirements.

Inherent with any flowing system are pressure-drop losses, both in the stack itself and in the associated plumbing between the stack and storage tanks. In designing a redox system, it is desirable to keep these pressure-drop losses to a minimum, since pumping power requirements are a direct parasitic energy loss to the redox system. Pressure-drop losses due to plumbing are unavoidable; however, significant decreases in pressure drop can be obtained through improved design of the flow ports, manifolds, and cavities in the cells composing the stack.

Shunt currents (ref. 3) are another parasitic energy loss to the system. Design parameters that decrease the pressure drop and hence the pumping power requirements tend to increase the shunt losses. When designing a specific system, trade-offs to minimize the sum of these parasitic energy losses obviously become necessary. This will be the subject of future reports. It is the purpose of this paper to present and compare pressure-drop data for cell designs with different combinations of port, manifold, and cavity dimensions. The effects of both the electrode structure and its dimensions on the pressure drop are also discussed. Knowing the pressure drop and design flow rate, the pumping power contribution to the overall system parasitic energy loss for a specific cell geometry and stack size can be calculated. This pumping power contribution is typically only a few percent of the total energy output for an entire system, with the sum of the pumping and shunt losses normally less than 5 percent.

BACKGROUND

A typical planform of a flow field frame assembly used in a redox stack is shown in figure 1. Reactant solution enters the flow field through an inlet primary manifold hole common to all cells in the stack, then flows

upward through an inlet port before entering the cell cavity. Here a gap is left between the flow field frame assembly and the electrode to form a secondary manifold which allows the reactant solution to spread out evenly before moving upward through the electrode. Flow leaves the cell through an exit secondary manifold, exit port, and exit primary manifold. Figure 2 depicts the parallel flow arrangement of single-cell components in a stack of redox cells. The gaskets and flow plate combine to form the flow-field frame assembly in each cell. The flow plate and gasket are identical except that the flow plate has an inlet and exit port to direct flow from the primary manifold both into and out of the cell cavity. Figure 3 shows an isometric view of one corner of the flow field frame assembly.

Under constant flow conditions, an increase in cross-sectional area or decrease in length in either or both the inlet or exit ports and manifolds will decrease the pressure drop. Different combinations of manifold, port, and cavity dimensions result in different pressure-drop values. The optimum combination exists when the sum of all parasitic pumping energy losses for a given combination is a minimum.

EXPERIMENTAL APPARATUS AND PROCEDURE

A single half-cell, mounted between two plastic blocks to simulate an operational cell cavity with a membrane on one side and terminal plate on the other side, was used to obtain the pressure-drop data. This half-cell rested diagonally in a stand so as to eliminate any head pressure difference between the inlet and outlet of the cell (as in fig. 4). The experiment working fluid chosen was water. The results were corrected for the viscosity appropriate for actual redox solutions. The water was stored in a glass reservoir and forced through the cell by nitrogen pressure from a continuous, regulated nitrogen gas supply. The pressure drop across the cell was measured by a calibrated pressure transducer (range, 0 to 103425 Pa $\pm$ 690 Pa (0 to 15 psid $\pm$ 0.1 psid)) the pressure from either the inlet or outlet tap being selected with a three-way valve. Line losses for this setup both to and from the cell were negligible compared with the magnitude of the actual cell pressure-drop loss. The measurements from the pressure transducer passed through a signal conditioner and were read on a digital voltmeter. Simultaneously, the flow rate from the cell outlet was measured using a graduated cylinder.

The experimental procedure consisted of first setting the nitrogen pressure to arrive at a desired flow rate. The inlet and outlet pressure readings were then taken, the difference being the pressure drop. The nitrogen pressure was then adjusted to arrive at a new flow rate and a subsequent pressure-drop value was measured. This procedure was followed for six different flow-field frame assemblies of various dimensions, both with and without electrodes.

RESULTS AND DISCUSSION

Two different cavity thicknesses were studied, namely, 0.125 and 0.250 cm. The three flow-field frame assemblies with cavities of 0.125 cm had inlet and exit flow-port depths of 0.075 cm, while the 0.250-cm cavity assemblies had flow-port depths of 0.200 cm. The three different flow-port widths for each cavity depth were 0.2, 0.4, and 0.7 cm. Flow rate and pressure-drop data were taken for these six different flow-field frame assemblies both with and without electrodes. The data are presented in figures 5 to 9.

The results follow a general pattern. For all three flow-port widths in figures 5 to 7, the pressure drop decreases as both the cavity and flow-port dimensions are increased. It also becomes evident that the porous carbon felt electrode causes roughly half the total cell pressure drop. This structure is 80 to 90 percent porous under normal conditions, but is compressed by 10 to 25 percent of its original thickness when placed in a cell cavity. The same electrode was used in each of the three 0.125-cm cell cavities, and the same pair of electrodes, which formed a double thickness, was used in each of the three 0.250-cm cell cavities. The same percentage of compression was used throughout. Figures 8 and 9 compare all the data without electrodes and all the data with electrodes, respectively. Both figures depict a pressure-drop increase as the port width decreases.

Table I shows the ideal pumping power of different size stacks for each flow-field frame assembly, assuming 100 percent efficient pumps. Since the pressure drop across a cell within a stack is independent of the number of cells per stack due to parallel cell flow, the pumping power is simply the product of the flow rate per cell, number of cells per stack, and the pressure drop. For the case of 0.125-cm cavity depth and both inlet and exit flow port dimensions of 0.7 by 0.075 cm, the appropriate curve in figure 7 shows a pressure drop of 4.8 psid at a flow rate of 300 ml/min. Correcting for the average actual solution viscosity of 1.55 centistokes, the ideal pumping power for a single cell becomes 0.26 W. Taking into account both redox solutions and a stack consisting of 40 cells, the system ideal pumping power as seen in table I becomes 21 W. Data in the upper right-hand corner of this table were unattainable for the flow-field frame assemblies under test because of the limit on available nitrogen pressure. These pumping power requirements contribute 5 percent or less to the overall parasitic energy loss for a particular cell geometry and stack size.

CONCLUDING REMARKS

The pressure drop for a particular cell geometry is composed of two contributing factors. The first is the actual dimensions of the flow port, manifold, and cavity. An increase in cross-sectional area or decrease in length in any or all of the above causes a decrease in pressure drop. The second factor is compression of the electrode. This carbon felt structure is 80 to 90 percent porous, and when compressed in a cell cavity it generally comprises half the total cell pressure drop. Depending on specific system requirements and shunt current trade-offs, the flow port, manifold, and cavity dimensions can all be adjusted to arrive at almost any cell geometry. The pumping power contribution to the overall system parasitic energy loss can be found simply by knowing the design flow rate and subsequent pressure drop. The most desirable cell geometry is the one that generates the minimum sum of both pumping power and shunt current parasitic energy losses.

REFERENCES

1. Thaller, Lawrence H.: Redox Flow Cell Energy Storage Systems. DOE/NASA/1002-79/3; NASA TM-79143, 1979.
2. Prokopius, Paul R.: Model for Calculating Electrolytic Shunt Path Losses in Large Electrochemical Energy Conversion Systems. NASA TM X-3359, 1976.
3. Workshop on Electrodes for Flowing Solution Batteries - Summary Report. EPRI WS - 79-192, SRI International, 1981.

TABLE I. - PUMPING POWER PER STACK AS CALCULATED FROM FLOW STUDIES

[Average solution viscosity, 1.55 cS; 929 cm^2 (1 ft^2) cell]

Cavity thickness, cm	Flow port dimensions, cm	Ideal pumping power, W								
		Flow rate per cell to each electrode, ml/mm								
		[a]150			[b]300			[c]450		
		Cells/stack			Cells/stack			Cells/stack		
		20	40	80	20	40	80	20	40	80
0.125	0.2x0.075	5.2	10	21	----	----	--	----	--	--
	.4x0.075	3.0	6.0	12	14	27	55	----	--	--
	.7x0.075	2.5	4.9	9.8	10	21	41	24	48	96
0.250	0.2x0.200	1.8	3.6	7.3	8.5	17	34	22	45	90
	.4x0.200	1.3	2.7	5.3	5.4	11	22	12	25	49
	.7x0.200	.96	1.9	3.8	3.8	7.7	15	9.0	18	36

[a]Typical discharge stoichiometric flow rate at ~80% DOD, 50 mA/cm^2.
[b]Typical discharge stoichiometric flow rate at ~80% DOD, 100 mA/cm^2.
[c]Typical discharge stoichiometric flow rate at ~90% DOD, 75 mA/cm^2.

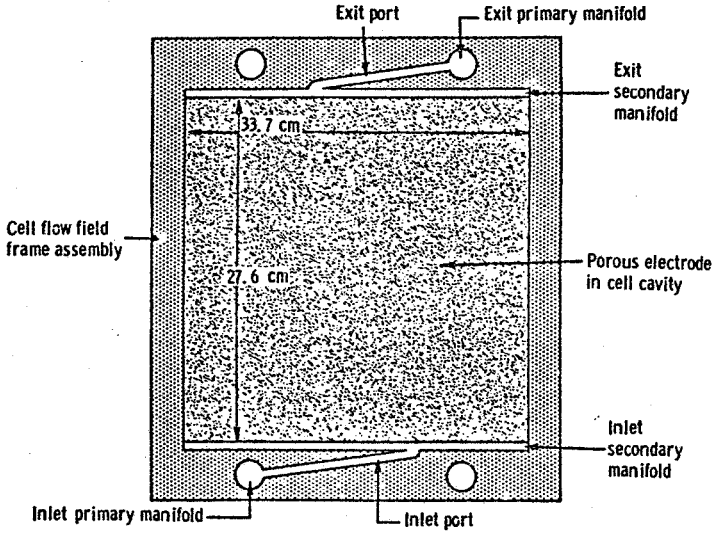

Figure 1. - Planform of cell flow field frame assembly.

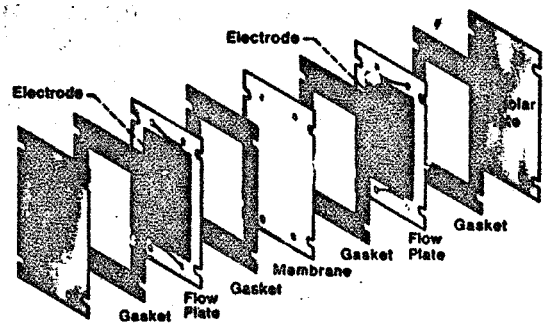

Figure 2. - Redox stack and single cell components.

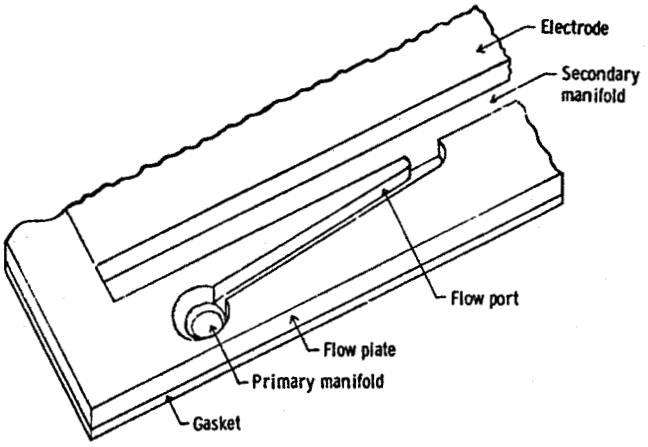

Figure 3. - Corner isometric view of flow field frame assembly with electrode.

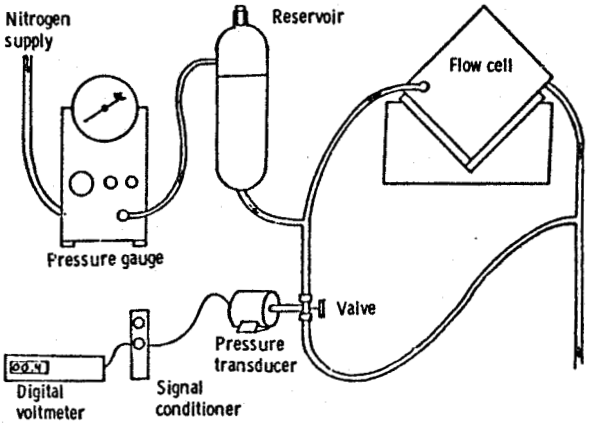

Figure 4. - Laboratory setup for determining cell pumping power.

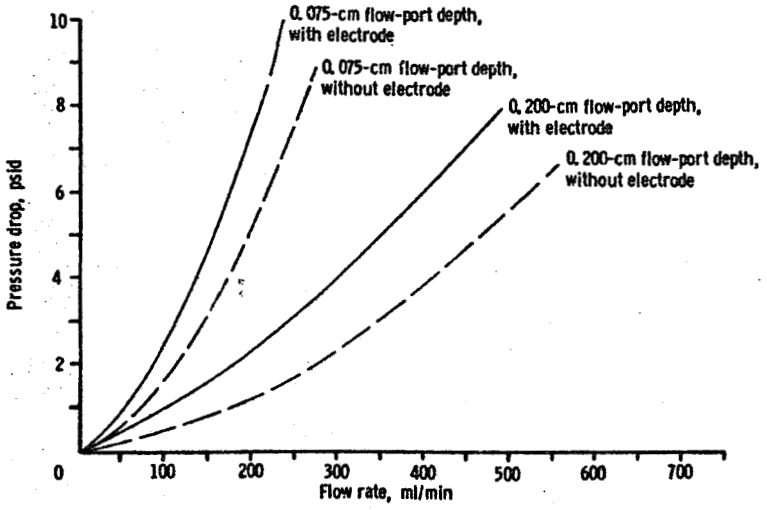

Figure 5. - Pressure drop versus flow rate for 929-cm^2 cell with 0.2-cm flow-port width.

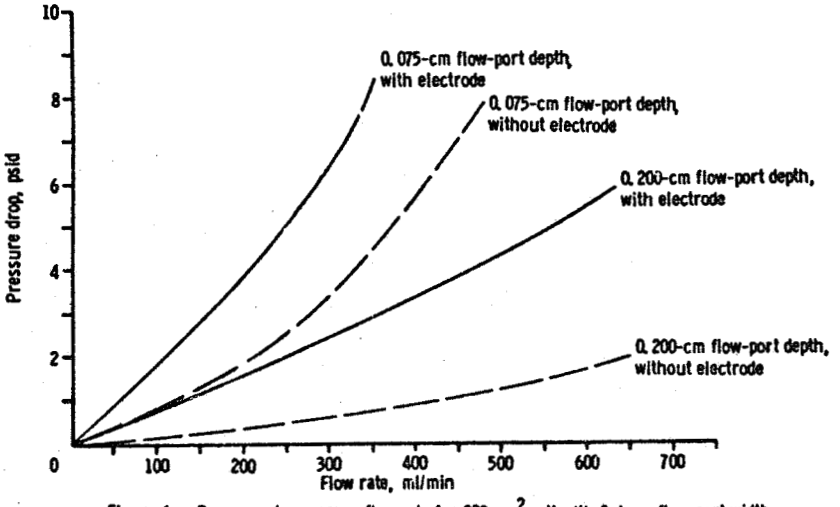

Figure 6. - Pressure drop versus flow rate for 929-cm^2 cell with 0.4-cm flow-port width.

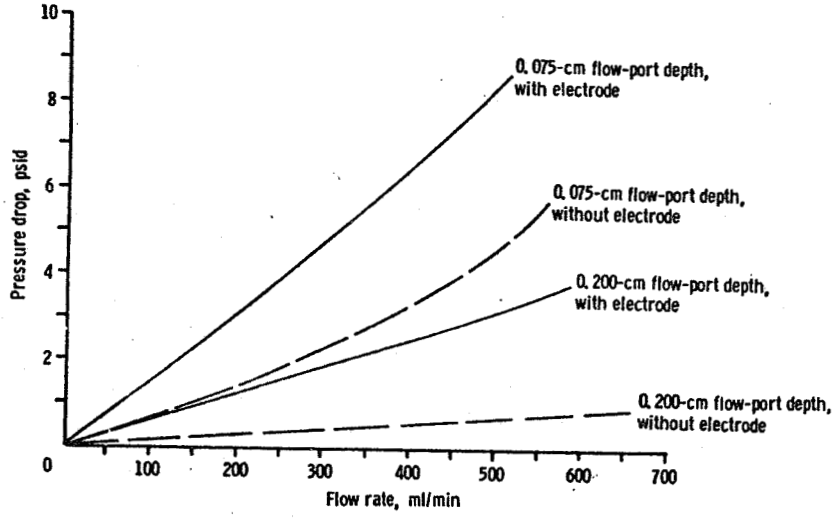

Figure 7. - Pressure drop versus flow rate for 929-cm^2 cell with 0.7-cm flow-port width.

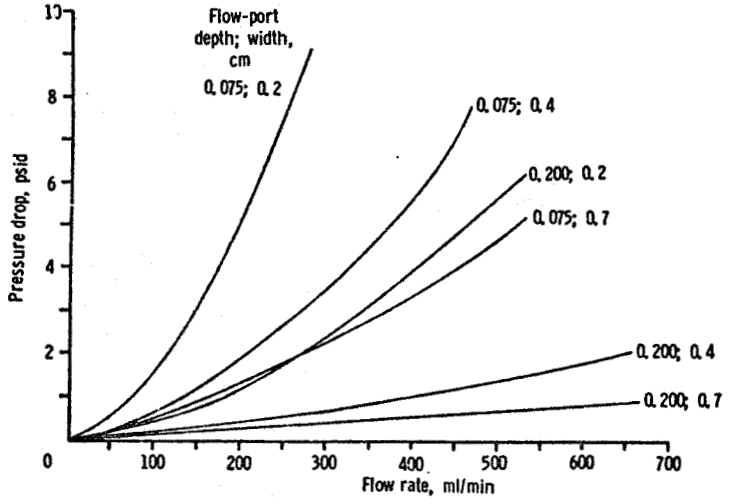

Figure 8. - Pressure drop versus flow rate for cell without electrodes.

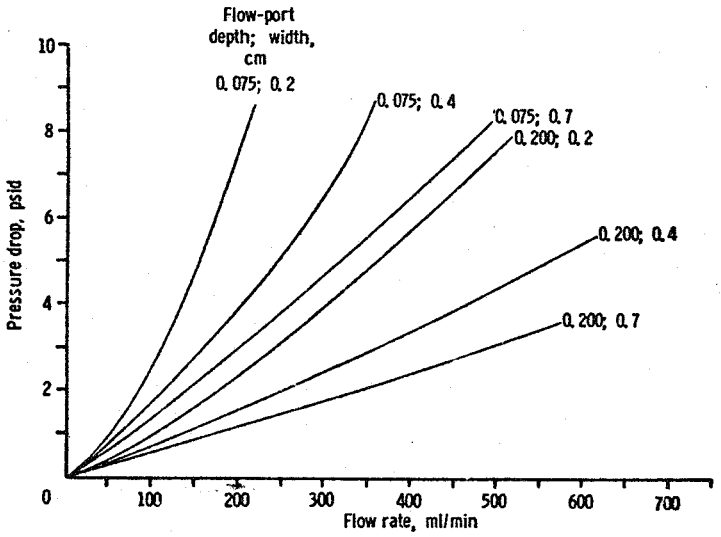

Figure 9. - Pressure drop versus flow rate for cell with electrodes.

END

DATE

FILMED

SEP 23 1981